Speckle variance optical coherence tomography for imaging microcirculation

D. Klawitter, D. Hillmann, M. Pieper, P. Steven, J. Wenzel, and G. Hüttmann

***Abstract*—Non-invasive flow detection and *in-vivo* measurement are one of the most requested clinical applications for medical imaging modalities to investigate vascular pathologies and responsiveness to drug therapy. Implementing speckle variance calculation & visualization in a market-proven optical coherence tomography (OCT) system we demonstrate an angiography imaging algorithm that provides angle independent, depth-resolved flow measurement up to a capillary scale. The feasibility of quantitative flow analysis with speckle variance OCT (svOCT) is to be demonstrated by the evaluation with silicone phantom, animal and human probes, respectively. First results lead to the assumption that reliable access to quantified flow velocities with svOCT is not obtainable. However svOCT delivers high vascular contrast at minimal oversampling rates, being a simple implementation module and a beneficial extension to OCT systems in general.**

I. Introduction

Optical coherence tomography (OCT) has become one of the most promising medical imaging modalities generating depth-resolved, high resolution, *in-vivo*, 3D structural and functional data non-invasively over the last two decades. OCT uses coherence gating of backscattered light for tomographic imaging of tissue structure and can be described as a reflecting mode scanning confocal microscope (CM) using a coherent light source. Imaging contrast is provided by variations in tissue scattering due to inhomogeneities in the optical index of refraction. One of the biggest challenges in exploring novel clinical applications of OCT is to develop contrast mechanism that generate physiological information in addition to morphological structure. Consequently the ability to detect and quantify flow, if possible in support of 3D or even 4D visualization, is one of the most required specification of optical imaging modalities for medical research.

In the field of OCT two types of vascular imaging techniques have been established, those who visualize quantified flow and those that uncover vascular networks but essentially generate no quantitative flow information. Applications of the first type, as phase-resolved Doppler imaging, measure phase shifts evoked by moving scatterers in the observed tissue. The second type including speckle contrast (sc) and speckle variance (sv), respectively, use speckle fluctuations to identify microvasculature by calculating either the interframe contrast or the intensity variance of structural images [3].

To understand interframe speckle fluctuations a short review of laser speckle and its properties is presented. The advent of laser speckle theory is dated to the invention of laser in the 1960's. When laser light illuminates an irregular surface, the high coherence of the light generates a random interference effect. At first the new phenomenon was called "granularity", but soon renamed by the more popular expression "speckle" [1]. Fig. 1 shows a typical "speckle pattern" and its probability dense function (PDF). The PDF of the intensity I_{LS} of laser speckle is negative exponential and characterized by a maximum probability of I_{LS} = 0, leading to the well-known high contrast $C_I = \sigma_{I_{LS}}/\langle I_{LS}\rangle$ = 1. Here $\sigma_{I_{LS}}$ is the standard deviation of I_{LS}, $\langle I_{LS}\rangle$ is its mean.

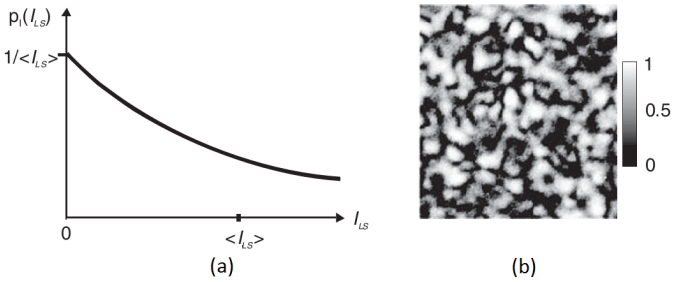

Fig. 1: (a) PDF of the intensity I_{LS} of laser speckle with $\langle I_{LS}\rangle$ as its mean. (b) Photographic image of a white piece of paper illuminated by coherent laser radiation shows fully developed laser speckle. Scale, $I_{LS}/\langle I_{LS}\rangle$ [2].

In the early years of lasers, speckle was mainly depicted as noise: it strongly affects resolution when laser light is used, much effort was directed towards reducing speckle in images formed in laser light. Later, researcher started to study speckle for its own sake and to developed practical applications of the effect. As a random phenomenon laser speckle can be described statistically. Although a detailed view on laser speckle statistics is beyond the scope of this paper, it is worth pointing out that the scale of the speckle pattern - the size of the individual speckles - has in general nothing to do with the structure of the surface producing it. It is defined only by the aperture of the beam optics used to observe the speckle pattern. If the speckle pattern is being observed by the human eye, it is the pupil of the eye that determines the speckle size. When

A. D. Klawitter, Medizinische Ingenieurwissenschaft, University of Luebeck; the work has been carried out at the Insitute of Biomedical Optics, University of Luebeck, Luebeck, Germany (e-mail: dominico.klawitter@miw.uni-luebeck.de

B. D. Hillmann is with Thorlabs HL AG, Luebeck, Germany (e-mail: hillmann@thorlabs.com)

C. M. Pieper is with Institute of Anatomy, University of Luebeck, Luebeck, Germany (e-mail: pieper@anat.uni-luebeck.de)

D. P. Steven is with Centre of Ophthalmology, University Hospital of Cologne, Cologne, Germany (e-mail: philipp.steven@uk-koeln.de)

E. J. Wenzel is with Institue of Pharmacology and Toxicology, University of Luebeck, Luebeck, Germany (e-mail: jan.wenzel@pharma.uni-luebeck.de)

F. G. Hüttmann is with Institute of Biomedical Optics, University of Luebeck, Luebeck, Germany (e-mail: huettmann@bmo.uni-luebeck.de)

an object moves, the generated laser speckle pattern changes, too. Concerning small motions of an object, the speckle move with the object, *i.e.* they remain correlated and the intensity values behave according to a Gaussian distribution.

A single speckle seems to "twinkle" like a star. This phenomenon is known under the expression "time-varying speckle". It is frequently obtained when living organisms are observed under laser light illumination. Probably the most important potential application of speckle fluctuation, first recognized by Stern in 1975, arises when they are induced by the flow of blood, precisely the movement of red blood cells (RBC) or erythrocytes.

Accordingly svOCT detects microvasculature by calculating the interframe intensity variance of structural images, where contrast is provided through different time-varying properties of fluid versus solid tissue components [4]. In other words svOCT dissociates static scattering from dynamic scattering components. In animal and human tissue the predominant cellular scattering factors are RBC. Thus blood vessels are typically visualized as highly scattering regions in standard OCT intensity images. Unfortunately interframe speckle variance calculation is strongly influenced by bulk tissue motion (BTM) leading to an artificial increased variance signal. This motion artefact can be reduced choosing optimized acquisition parameters [5]. Here we implement svOCT into a market-proven and commercial available OCT system and show its capability of simple and computational efficient access to microangiography. Furthermore its performance is evaluated by animal models, especially investigating the ability to quantify blood flow with a silicone phantom at different flow velocities.

II. Material and Methods

All measurements were performed with the Telesto Spectral-Domain OCT (SDOCT) imaging system from Thorlabs GmbH, Dachau, Germany. SDOCT is one of two embodiments known under the overall category of Fourier-Domain OCT (FDOCT). These methods are called "Fourier-Domain" because they detect the interference spectrum and do not require mechanical scanning of the reference path length in time. For this reason a SDOCT system with a broadband light source extracts spectral information from the interference signal by distributing different optical frequencies onto a high-speed, high resolution spectrometer (detector line-array) using a dispersive element. Thereby the information of a full depth scan (A-scan) can be measured within a single shot. Specifications of the Telesto imaging system are: center wavelength $\lambda_0 = 1325\ nm$, axial scan frequency $f_s = 5,5/28/91$ kHz, axial resolution (air / water) $\Delta z = 6,5\ \mu m$ / $4,9\ \mu m$, lateral resolution $\Delta x, y = 15\ \mu m$, optical power on sample $P = 3\ mW$, pixel per A-scan = 512, maximum imaging depth $d = 2.5\ mm$ and a maximum field of view (FOV) $l \cdot w \cdot d = 10 \cdot 10 \cdot 2,5\ mm^3$.

Speckle variance calculation was performed under use of an experimental software module based on LabVIEW (National Instruments, 2012, 64 bit, Austin, US). After installation of the software add-on to the working computer (Dell T5500, 4 x 2,13 Ghz, 12 GB DDR3 RAM, 500 GB HDD) and its operating system (Microsoft Windows 7 x64) the system was capable to process interframe speckle variance images (SV_{ijk}) of the structural OCT intensity (I_{ijk}) based on the following equation

$$SV_{ijk} = \sigma_I^2 = \frac{1}{N}\sum_{i=1}^{N}\left(I_{ijk} - \frac{1}{N}\sum_{i=1}^{N} I_{ijk}\right)^2 \qquad (1)$$

where the gate length N sets the number of B-scans used in the variance calculation, and *i,j,* and *k* are indices for the B-scan or frame, transverse, and axial pixels. Calculation of the A-scans yields complex OCT signal consisting of the absolute value and the phase. For structural intensity images only the absolute value will be represented on screen. Our software module allows several options to process speckle variance. Either the original OCT signal as input variable is linear (lin), logarithmized (log) or complex (com). After calculation of variance the output can be chosen as linear or logarithmized. Consequently there are six different in- & output variations: *lin - lin, lin - log, log - lin, log - log, com - lin* and *com - log*.

Although the software module provides averaging axially (averaging several A-scan-points) and along fast axis (oversampling of several A-scan-lines) the most sensitive scanning mode to detect microcirculation is along slow axis (oversampling of several B-scans). Caused by the slow flow velocities in capillaries of about 0.1 - 0.9 mm/s there must be a time gap between following B-scans of some microseconds. B-scans oversampling leads to adequate time gaps and image scaling stays constant. The methods consist of five studies:

1) silicone phantom (variance calculation)
2) silicone phantom (flow quantification)
3) animal model (mouse ear - microangiography)
4) animal model (mouse cranium - microangiography)
5) animal model (mouse cornea - microangiography)

For the phantom measurements a polymer tube embedded in silicone phantom with an inner diameter of 280 μm was filled with Intralipid 10 % (Baxter) to study variance calculation of different signal input and output visualization . The silicone was mixed with white nanoparticles to reach a similar level of scattering. A syringe pump generated various flow velocities from 0.135 to 8.9 mm/s to verify the potential of flow quantification.

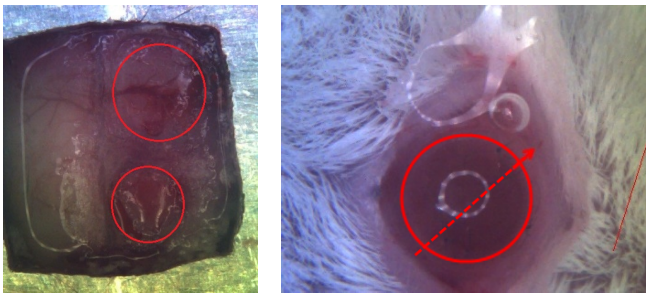

(a) (b)

Fig. 2: (a) Mouse cranium with cranial windows (red circles); (b) mouse eye with red arrow indicating the B-scan of Fig. 6 (a)and red circle representing the C-scan position in Fig. 6 (b).

The experiments with animal models consisted of measuring mouse ear, cranium and cornea. All mice had to be sedated. The mouse ear had to be depilated with creme so that the fine hairs could not irritate the image acquisition. To prevent the measurement from BTM the ear was taped on the sample stage. A second mouse with prepared cranial windows was obtained to uncover the cerebral vessel network, especially challenging the question of vasculature imaging through the intact skull (Fig. 2(a)). A third mouse with induced neovascular defects, caused by implanted suture into cornea, was anaesthetized and fixation of the eye lid was attended (Fig. 2(b)). Stored into a customized mouse holder with temperature controlled bottom and artificial respiration support the measurements could be accomplished. All measurements were performed with a scan frequency of 28.000 Hz.

III. Results and Discussion

A. Silicone phantom

1) Evaluation of different variance calculation methods: Fig.3 represents a typical B-scan of the silicone phantom with polymer tube embedded. Here the intralipid solution is completely static and Brownian motion is dominant. Time stacks of 100 frames at the same location were acquired and the region of interest (RIO) was set as circular region inside the polymer tube (Fig 3 (b)). In Table I we see the overall mean, minimum and maximum at the ROI of all frames for the six different calculations. In comparison no significant difference between the calculation variations can be obtained. However the main effect of svOCT can be observed. The contrast between static and dynamic scattering components of tissue increases so that fluids and their canalization can clearly be identified.

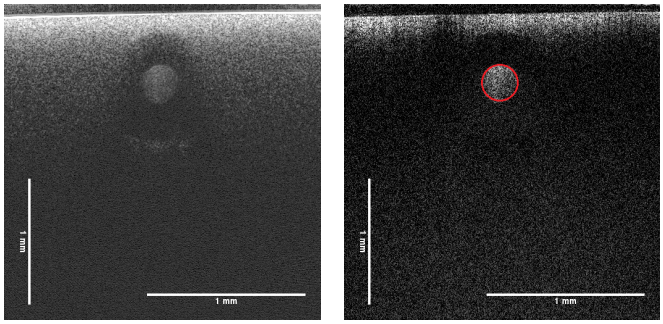

(a) (b)

Fig. 3: B-scan of silicone phantom with polymer tube embedded (a) mean intensity image and (b) variance image of *lin - lin* calculation with ROI as red circle (N = 3, FOV = $2 \cdot 2.5\ mm$).

TABLE I: Variance calculation results

in	out	mean	min	max
lin	lin	3.777	1.555	5.588
lin	log	3.802	2,010	5.789
log	lin	3.794	1.401	5.605
log	log	3.811	1.267	5.621
comp	lin	3.820	1.549	5.611
comp	log	3.764	1.721	5.633

Calculating michelson contrast ($K_M = I_{max} - I_{min} / I_{max} + I_{min}$) between the ROI inside the polymer tube and another ROI outside at the same depth level reveals K_M= 0.033 for a normal intensity image and K_M = 0.14 for a variance image.

2) Evaluation of quantified flow measurements: Using the syringe pump to generate flow rates of 0,1 ,2 ,4 , 5, 10, 15, 20, 25, 30 $\mu l/min$. Variations of the speckle variance signal were investigated. Analysing the circular ROI (red circle Fig. 3 (b) inside the polymer tube and its lateral progress a dependency of the variance signal to the velocity of RBC has to be denied. A dependency should be reflected in a dramatic change of the maximum variance signal but neither the mean nor the maximum signal is altering (Fig. 4). In this case the results of Barton 2005 [6] can not be reproduced. She showed a depth-resolved flow profile and increased flow signal due to rising flow velocities with svOCT.

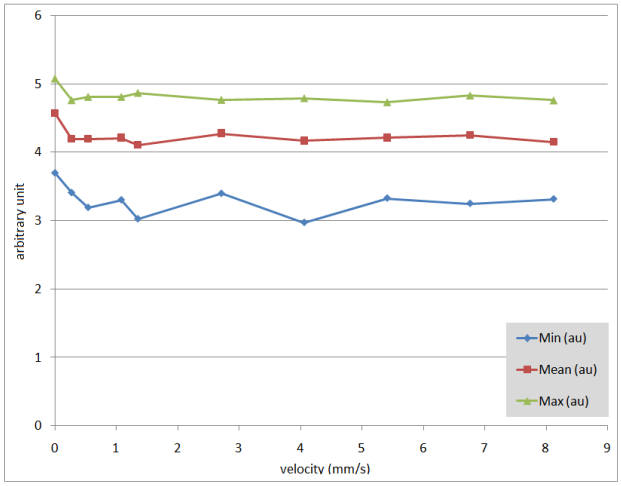

Fig. 4: Minimum, mean and maximum values of speckle fluctuations inside the RIO in relation to the flow velocity (see Fig. 3 (b)).

B. Animal model

1) Mouse ear: In Figure 5 (a) we see delimited layers of a

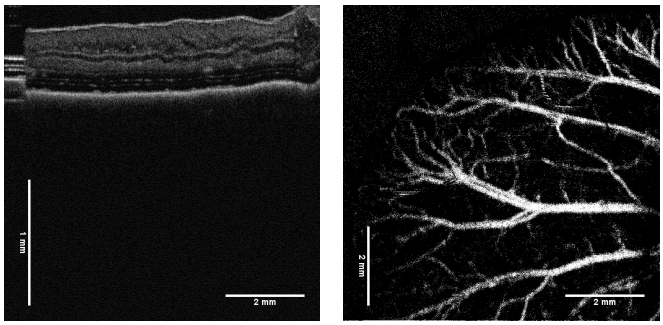

(a) (b)

Fig. 5: Mouse ear *in-vivo* (a) B-scan of mean intensity and (b) vessel network detected by MIP of variance images (N = 3, FOV = $8 \cdot 8 \cdot 2.5\ mm$).

we see delimited layers of a mouse ear in a mean intensity B-scan. Large field of view of the Telesto SDOCT allowed to image almost the whole mouse ear without the need to stitch several pictures. MIP of the speckle variance allow to uncover the complex vessel network (Fig.5 (b)) and enables investigation of vessel localization, ramification and diameter.

2) Mouse cranium: Is it possible to depict vessel through the transparent cranium ($\approx 200\,\mu m$) of a mouse *in-vivo* with svOCT when vessels are visible to the naked eye? The answer to this question can be seen in Fig. 6 (b), where vessels can clearly be identified not just inside the cranial windows but also next to them with intact cranium. This advantage allows scientist to measure a living subject repeatedly without the need to open the skull and consequently dispatch the animal.

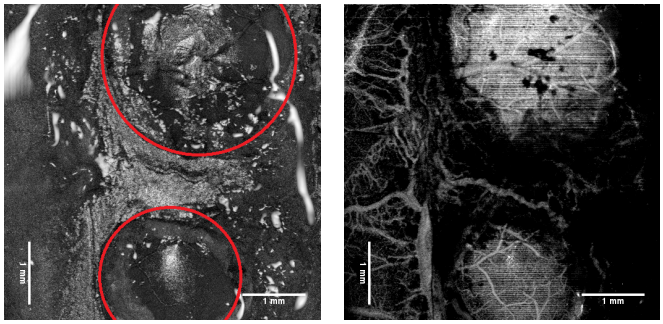

(a) (b)

Fig. 6: (a) C-scan of mean intensity images showing mouse cranium with two cranial windows represented as red circles and (b) MIP of variance C-scans (N = 3, FOV $= 5 \cdot 5 \cdot 2.5\ mm$).

3) Mouse cornea: Neovascular defects in cornea are one of the clinical important reasons for corneal opacity. Therefore the detection and visualization of such growing vessels in cornea is a relevant field of medical research. In Figure 7 (a) we see a B-scan of mean intensity through a mouse eye *in-vivo* (see also Fig. 2(b)). The white line indicates the sections where the MIP of variance images was processed. Invisible for light microscopy the corneal vessels are disclosed by svOCT (Fig. 7 (b)).

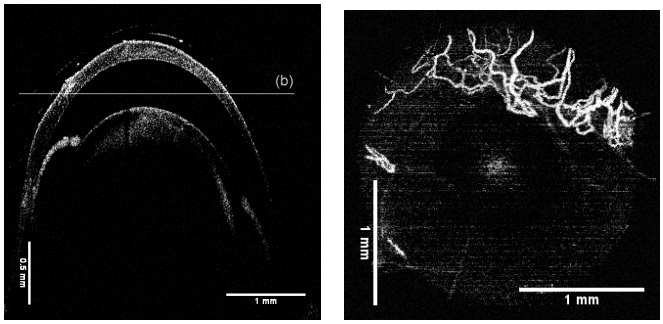

(a) (b)

Fig. 7: Mouse eye (a) B-scan of mean intensity and (b) MIP of several variance C-scans showing corneal vasculature (N = 2, FOV $= 4 \cdot 4 \cdot 2.5\ mm$).

IV. Conclusions

In recapitulation of previous experiments we can state svOCT with the Telesto SDOCT is a fast imaging technique to detect microcirculation and structural information at the same time. To uncover vessel networks C-scan or En-Face-scans must be calculated of variance B-scan stacks. A simple way to attain 2D angiography images is a maximum intensity projection. Experiments with the silicone phantom showed neither a significant dependency of variance to different calculation algorithms nor to varying flow velocities. With no possible differentiation of flow velocities quantification of perfusion is out of reach. We showed the feasible imaging of vessel networks in physiological tissue of animal probes *in-vivo*. Practical clinical application could be the investigation of corneal neovascular defects.

Caution must be practised in the analysis and interpretation of OCT angiograms due to possible intensity changes by increased RBC velocity, increased hematocrit or alternating RBC orientation. Optimization of svOCT imaging parameters as resolution and frame rate will lead to an improvement in capillary detection. In situations where tissue motion is high, the field of view or frame rate during acquisition must be optimized to keep interframe displacements to less than the beam waist radius.

To summarize, svOCT is a highly sensitive, angle independent, endogenous-contrast vascular imaging technique that provides best results in tissue with low BTM. Unlike DOCT imaging svOCT is not able to provide information about the flow orientation. However, svOCT delivers high vascular contrast at minimal oversampling rates, visualizing flow even at molecular motion level. Speckle analysis in OCT images could be advantageous to DOCT because it is sensitive to motion normal to the incident beam, eliminating the need for phase-sensitive detection. A combination of svOCT and DOCT could resolve problems on both sides of optical coherence angiography. In conclusion, svOCT is an microangiography imaging method with simple implementation and an advantage for clinical diagnostic, as well as a beneficial extension for OCT system in general.

References

[1] J.D. Ridgen and E.I. Gordon, *The granularity of scattered optical maser light*, Proceedings of the IRE **50**, 1962

[2] W.J. Drexler and J.G. Fujimoto, *Optical Coherence Tomography*, Springer Berlin Heidelberg, 2008.

[3] J.D. Briers, *Laser speckle contrast imaging for measuring blood flow*, Optica Applicata, Vol.XXXVII, No. 1-2, 2007

[4] A. Mariampillai et al., *Speckle variance detection of microvasculature using swept-source optical coherence tomography*, OPTIC LETTERS, Vol. 33, No. 13, 2008

[5] A. Mariampillai et al., *Optimized speckle variance OCT imaging of microvasculature*, OPTICS LETTERS, Vol. 35, No. 8, 2010

[6] J.K. Barton, S. Stromski, *Flow measurement without phase information in optical coherence tomography images*, OPTICS EXPRESS, Vol. 13, No. 14, 2005